HIGH-SPEED JETS IMPINGING ON THE EARTH'S MAGNETOSPHERE: A STATISTICAL STUDY ON WHERE AND WHEN THEY OCCUR

Laura Vuorinen, Heli Hietala
Dept. of Physics and Astronomy, University of Turku, Finland
email: lakavu@utu.fi

OVERVIEW

High-speed jets (HSJs) are regions of plasma in the magnetosheath (Fig. 1) that move faster towards Earth than the surrounding plasma. If they collide into the magnetopause, the impacts can trigger processes that can affect the Earth's magnetic field and, for example, cause auroras.

We statistically study the occurrence of these jets in the subsolar magnetosheath using 2008–2011 measurements from the five THEMIS spacecraft and OMNI solar wind data. We find that the occurrence rate of jets increases as the angle between the bow shock normal and the interplanetary magnetic field (IMF) decreases. This corresponds to the location of the foreshock region upstream, suggesting that foreshock phenomena are responsible for jet formation.

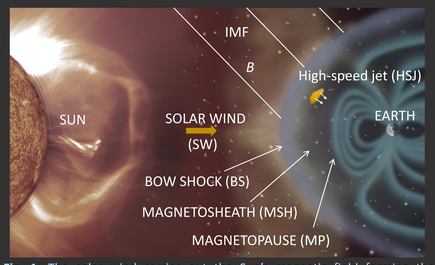

Fig. 1: The solar wind carries out the Sun's magnetic field forming the interplanetary magnetic field (IMF). The solar wind is first slowed down and deflected by the Earth's bow shock, which is formed by the encounter of the supersonic solar wind and the Earth's magnetic field. The deflected plasma flows between the bow shock and the boundary of the Earth's magnetosphere (magnetopause), in the magnetosheath. Jet size is usually larger perpendicular to the flow direction with this width being comparable to Earth radius (Plaschke et al. 2016). The image is not to scale.

1. MOTIVATION

- Testing a model of a jet generation mechanism based on bow shock ripples that are inherent to the quasi-parallel bow shock
- How often do these jets occur?

2. INTRODUCTION

- Plaschke et al. (2013): in the subsolar MSH, jets occur predominantly when the cone angle $\alpha \in [0^o, 90^o]$ between the IMF line and the Earth-Sun line (the X_{GSE}-axis) is small ($\alpha < 45^o$)
- The cone angle α approximates the angle θ_{Bn} between the bow shock normal and the IMF
- $\theta_{Bn} < 45^o$: Quasi-parallel part of the bow shock
  $\theta_{Bn} > 45^o$: Quasi-perpendicular part of the bow shock
- A foreshock region is formed upstream of the quasi-parallel shock by the interaction of the solar wind with particles reflected from the shock. The turbulence increases with smaller θ_{Bn}.
- Hietala et al. (2009): jet formation mechanism based on bow shock ripples that are inherent to the quasi-parallel shock
- The locations of the quasi-parallel and quasi-perpendicular areas depend on the IMF orientation as shown in Fig. 2.

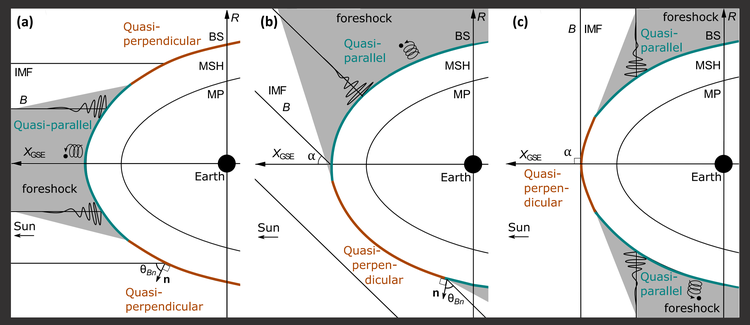

Fig. 2: The approximate locations of the quasi-parallel and quasi-perpendicular parts of the bow shock for the IMF cone angles (a) $\alpha = 0^o$, (b) $\alpha = 45^o$ and (c) $\alpha = 90^o$. The quasi-parallel and quasi-perpendicular areas are color-coordinated. The turbulent foreshock region upstream of the quasi-parallel area is highlighted in gray color. $R = (Y_{\mathrm{GSE}}^2 + Z_{\mathrm{GSE}}^2)^{1/2}$ is the cylindrical coordinate.

3. DATA

Data set:

- THEMIS spacecraft measurements from 2008–2011
- 9,003,850 MSH observations in a Sun-centered 30° wide cone with its tip at Earth
- 2,859 of those were HSJs (see Fig. 3)
- SW data: averages of OMNI measurements from the five preceding minutes

Selection criteria for jets:

- Dynamic pressure of a HSJ in the anti-sunward direction (the $-X_{\mathrm{GSE}}$-direction) is over half of the SW dynamic pressure (assuming protons only):
  $P_{\mathrm{dyn,MSH},X} = \rho_{\mathrm{MSH}} v_{\mathrm{MSH},X}^2 > \frac{1}{2} P_{\mathrm{dyn,SW}} = \frac{1}{2} \rho_{\mathrm{SW}} v_{\mathrm{SW}}^2$
- t_0 is the moment of highest ratio between MSH and SW dynamic pressures in the jet and the time of the jet observation in our data set
- The full list of criteria in Plaschke et al. (2013)
- An example jet in Fig. 4

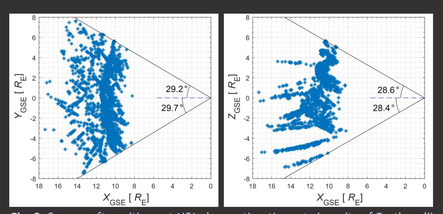

Fig. 3: Spacecraft positions at HSJ observation times t_0 in units of Earth radii (R_E). Jets were observed on the whole width of the 30° observation cone but there were gaps due to the spacecraft orbits. The $-Y_{\mathrm{GSE}}$-axis points in the direction of Earth's orbital motion and the Z_{GSE}-axis is perpendicular to the ecliptic plane and points north.

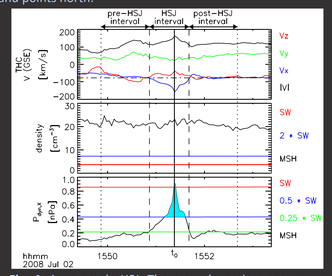

Fig. 4: An example HSJ. The max. dynamic pressure was over 4 times that of its surroundings and larger than the SW dynamic pressure. Figure from Hietala et al. (2013).

4. METHODS

- Three zones by cone angles:
  $\alpha \in [0^o, 30^o[$, $\alpha \in [30^o, 60^o[$ and $\alpha \in [60^o, 90^o]$
- We normalize the HSJ distribution by the MSH distribution to account for the time spent under certain conditions
- 2D maps: model BS by Merka et al. (2005) and model MP by Shue et al. (1998), all positions normalized to the mean $P_{\mathrm{dyn,SW}}$ of each zone

To measure whether a jet is on the quasi-parallel or the quasi-perpendicular area, we form a new coordinate system (Fig. 5):

- Position vector: $\boldsymbol{r} = R_X \boldsymbol{x} + R_{||}\, \boldsymbol{b}_{||} + R_\perp \boldsymbol{b}_\perp$, where $\boldsymbol{x}$ is the X_{GSE}-axis unit vector and $\boldsymbol{b}_{||}$ is an unit vector parallel to the YZ-projection of the IMF line
- $\boldsymbol{b}_{||}$ points towards the side that the cone angle α opens to when α is facing sunward
- The quasi-parallel area is mostly on the side where $R_{||} > 0$ as θ_{Bn} gets smaller with increasing $R_{||}$ because of the bow shock curvature

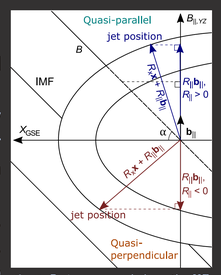

Fig. 5: $R_{||}$ is measured along the YZ-projection of the IMF line ($B_{||,\mathrm{IMF}}$).

5. RESULTS

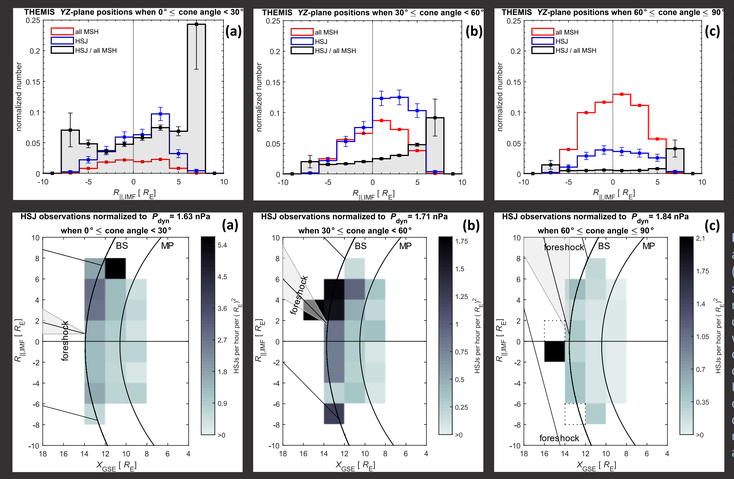

Fig. 6: The distributions of HSJs (blue), all MSH observations (red) and HSJ/all (black) as a function of $R_{||}$ in units of Earth radii ($R_E = 6{,}371$ km). The histograms of different IMF cone angle ranges sum up to 1. The error bars for HSJs and all MSH observations are 95% binomial proportion confidence intervals with the normal approximation. The error bar for HSJ/all MSH distribution was calculated as maximum deviations of the calculated HSJ and MSH distributions.

Fig. 7: The number of HSJs observed by a spacecraft per hour per R_E^2 in the (X_{GSE}, $R_{||}$)-plane with different IMF cone angle ranges. The positions are normalized to the mean solar wind dynamic pressures of each zone. The white squares have < 500 MSH observations. The dashed squares contain ≥ 500 MSH observations but 0 HSJs. The IMF lines on the left correspond to the middle value of the cone angle range and the cones represent the whole range of cone angles.

The normalized HSJ/all MSH (black and filled with gray) histograms in Fig. 6 show us:

- More jets with lower cone angles
- Increasing trend of jet occurrence for increasing $R_{||}$ in Fig. 6a and Fig. 6b
- Increased occurrence rates on the edge of the observation area in Fig. 6c corresponding to the expected location of the quasi-parallel area

The 2D maps in Fig. 7 show us:

- Jets were observed more often close to the bow shock than near the magnetopause
- Jets are generally most common around the areas downstream of the expected foreshock regions with small θ_{Bn}

6. SUMMARY AND CONCLUSIONS

- In the subsolar magnetosheath, high-speed jets occur predominantly on the quasi-parallel part of the bow shock
- Jet occurrence rate increases as the angle between the bow shock normal and the IMF decreases, suggesting that foreshock phenomena are responsible for jet formation
- Jets are most often detected close to the bow shock which suggests they are formed there and propagate towards the magnetopause
- Spacecraft observe at most around 5 jets in an hour per R_E^2
- Outlook: 3D simulations, jets in other shock environments, e.g. at other planets in the Solar System

REFERENCES

Hietala et al., *Phys. Rev. Lett.* 103, 245001, (2009)
Hietala et al., *J. Geophys. Res. Space Physics*, 118, 7237–7245, (2013)
Merka et al., *J. Geophys. Res.*, 110, A04202, (2005)
Plaschke et al., *Ann. Geophys.*, 31, 1877-1889, (2013)
Plaschke et al., *J. Geophys. Res. Space Physics*, 121, 3240–3253, (2016)
Plaschke et al., *Space Sci. Rev.* 214: 81, (2018)
Shue et al., *J. Geophys. Res.*, 103(A8), 17691–17700, (1998)

ACKNOWLEDGEMENTS

Fig. 1 courtesy of ESA & NASA and illustrated by Steele Hill.

We acknowledge NASA contract NAS5-02099 for use of data from the THEMIS Mission. The THEMIS and OMNI data are publicly available via, e.g., spedas.org.

This work was supported by the Turku Collegium of Science and Medicine.